JOURNAL OF COMPUTATIONAL PHYSICS 82, 413–428 (1989)

Flux-Corrected Pseudospectral Method for Scalar Hyperbolic Conservation Laws

B. E. McDONALD

Ocean Sensing and Prediction Division,
Naval Ocean Research and Development Activity,
Stennis Space Center, Mississippi 39529

Received November 30, 1987; revised June 21, 1988

The pseudospectral method has under-used advantages in problems involving shocks and discontinuities. These emerge from superior accuracy in phase and group velocities as compared to finite difference schemes of all orders. Dispersion curves for finite difference schemes suggest that group velocity error typically outranks Gibbs' error as a cause of numerical oscillation. A flux conservative form of the pseudospectral method is derived for compatibility with flux limiters used to preserve monotonicity. The resulting scheme gives high quality results in linear advection and shock formation/propagation examples. © 1989 Academic Press, Inc.

INTRODUCTION

Spectral methods for inviscid flow problems involving shocks have been developed at a slower rate than for problems where discontinuities are absent. This has been recognized explicitly [1] and implicitly [2] in papers taking a broad view of the subject. It is the purpose of the present paper to show how the pseudospectral method [3] can be substituted for a finite difference scheme in flux corrected transport (FCT) calculations, and to show why the results are better. The FCT method [4, 5] is effectively a local, nonlinear filter used to control numerical oscillations near shocks and steep gradients.

The flux correction method used here employs the Zalesak flux limiter [5]. In this approach, two arbitrary schemes are cast in conservation form: one of high order (pseudospectral), and the other monotone (e.g., first order upwind). A "flux correction" filter effectively assigns a local weight factor to fluxes from each scheme. The method adopts the form of the high order scheme in smooth regions. In locations where monotonicity could be violated by the high order scheme, weighting is shifted in favor of the low order fluxes. Comparisons made elsewhere with analytic solutions show that the accuracy of the overall method generally increases with the order of the high order scheme [6, 7].

Zalesak carried out an FCT pseudospectral calculation [6] for linear advection which gave results of higher quality than those from finite difference schemes up to sixteenth order in space. The method, however, was formulated in a fashion that

0021-9991/89 $3.00

did not take advantage of fast Fourier transforms (FFTs). Taylor *et al.* [8] gave *results* of a pseudospectral shock calculation using FFT's. They chose a Chebyshev polynomial expansion in space, appending the Boris–Book flux limiter [4] as a postprocessor to control oscillations at each time step. This involved adding global second order diffusion, followed by flux limited antidiffusion. Properties of the method itself were not discussed in that work, nor were the effects of wave propagation through the nonuniform grid required for the Chebyshev expansion. This work takes a different approach to discretization and flux limiting and *does* take advantage of FFT's.

Depending on the physical problem under consideration, high order methods may have advantages over shock capturing methods of the Godunov type [9–11]. These methods discretize variables into piecewise polynomial sections (allowing discontinuities between sections or subsections) and use gasdynamic Riemann solutions to advance a step in time. After the timestep, the solution is projected onto the original basis as input to the next timestep. These methods can yield accurate results for shocks, but their complexity increases greatly with order. In regions where the flow may be dominated by linear advection, these methods give results equivalent to those of low to moderate order finite differences.

The High Order Scheme: Pseudospectral

We will work with a model problem for a scalar hyperbolic equation in one dimension:

$$\partial_t v + \partial_x \phi(v) = 0. \tag{1}$$

This equation leads straight to the conservation of $\int v\,dx$ and to the preservation of monotonicity (extrema can be neither created nor enhanced). The method developed in this paper may be modified to include systems of equations by replacing $\phi(v)$ by the appropriate advective flux $\mathbf{u}v$, and using suitable donor cell fluxes in Eq. (10) below.

The pseudospectral method evaluates the x derivative in (1) by performing an FFT, then evaluating derivatives analytically before the inverse FFT. Let the finite difference grid be

$$x_j = j \cdot \delta x, \qquad j = 1, 2, ..., N, \tag{2}$$

and let ϕ be represented in space by Fourier series:

$$\phi = \sum_k \hat{\phi}(k) \exp(ikx). \tag{3}$$

We will assume periodic boundary conditions on all variables for simplicity. Other boundary conditions can, of course, be included at the expense of altering the selection of admissible modes. One can use the identity

$$\sin\left(\frac{k\,\delta x}{2}\right) = \frac{e^{ik\delta x/2} - e^{-ik\delta x/2}}{2i} \tag{4}$$

to express the x derivative of (3) as

$$\partial_x \phi = \sum_k \frac{k}{2} \hat{\phi}(k) \frac{e^{ik(x+\delta x/2)} - e^{ik(x-\delta x/2)}}{\sin(k\,\delta x/2)}. \tag{5}$$

One recognizes this as the difference between a function shifted forward half a grid cell and the same function shifted backward half a grid cell. This suggestive result leads directly to the conservative flux form given in (6) and (7) below.

For the discretization of (1) in time, we will use the leapfrog trapezoidal scheme [12] with step δt between time levels. This scheme can be thought of as a predictor–corrector with the predictor being a leapfrog step from time level $n-1$ to a provisional level $n+1^*$ using spatial derivatives evaluated at level n. Then the provisional level $n+1^*$ is averaged with n to yield a provisional level $n+\frac{1}{2}^*$. The trapezoidal corrector is a step from n to $n+1$ using spatial derivatives evaluated at $n+\frac{1}{2}^*$. This provides second order accuracy in time, while damping the computational mode ("odd–even" Nyquist frequency oscillations in space and/or time), which could interfere with the flux corrector used here.

Employing (5) in the time-discretized equation (1) leads to the conservative flux form for the pseudospectral method:

$$v_j^{n+1} = v_j^n - F_{j+1/2}^{n+1/2} + F_{j-1/2}^{n+1/2}, \tag{6}$$

where superscripts indicate time level and

$$F_{j+1/2}^{n+1/2} = \frac{\delta t}{\delta x} \sum_{k \neq 0} \hat{\phi}^{n+1/2}(k) \left(e^{ik\delta x/2} \frac{k\,\delta x/2}{\sin(k\,\delta x/2)} \right) e^{ikx_j}. \tag{7}$$

A flux form of this type seems to have been recognized only recently as a possible ingredient in a monotonicity preserving scheme [13, 14]. The leapfrog trapezoidal time advancement scheme used here is stable for Courant number $\varepsilon = |u\,\delta t/\delta x|_{\max} \leqslant 2^{1/2}/\pi = 0.45$, where u is the characteristic speed (see (9) below). For simple leapfrog advancement, the limit is $1/\pi$. The $k=0$ mode has been dropped from (7) for an important reason. Different additive constants in high and low order fluxes would lead to a meaningless bias in the flux correction process, which assigns a physical interpretation of intergridpoint transport to the difference between high and low order fluxes. We remove the spatial mean from the high order flux (7) by excluding $k=0$, and from the low order flux by computing the average and subtracting it.

The Low Order Scheme: Monotone Upwind

A convenient first order monotone scheme [7] for (1) is upwind differencing with the differencing direction defined by a variable

$$w_{j+1/2} = (\phi_{j+1} - \phi_j) \cdot (v_{j+1} - v_j), \tag{8}$$

whose sign is that of the characteristic speed u somewhere on the interval (v_j, v_{j+1}), where

$$u = \frac{d\phi}{dv}. \tag{9}$$

We define first order fluxes

$$f_{j+1/2} = \begin{cases} \phi_j \, \delta t/\delta x, & w_{j+1/2} \geqslant 0 \\ \phi_{j+1} \, \delta t/\delta x, & w_{j+1/2} < 0, \end{cases} \tag{10a}$$

and remove the spatial average,

$$f_{j+1/2} \to f_{j+1/2} - \langle f \rangle. \tag{10b}$$

When equations are given without superscripts, it is understood that all variables are evaluated at the same time level. The removal of the mean value in (10b) has no effect on the low order update (11), but is necessary for compatibility with (7) in the flux correction process. A monotone first order update accounting for reversals in the sign of u is

$$v_j^{n+1'} = v_j^n - f_{j+1/2}^n + f_{j-1/2}^n. \tag{11}$$

This provisional update to time level $n+1'$ is set aside for correction as described below. The above scheme is monotone for $\varepsilon \leqslant \frac{1}{2}$. This allowed Courant number is smaller by a factor of two than that for stability alone. The extra factor of two allows for monotonicity preservation when u is compressive at an extremum of v [7].

Flux Correction: A Nonlinear Filter

The next step is to construct a set of "flux corrections"

$$\delta f_{j+1/2}^{n+1/2} = F_{j+1/2}^{n+1/2} - f_{j+1/2}^n \tag{12}$$

and filter them with a flux limiter to prevent creation or enhancement of extrema. For problems of higher than one dimension, flux limiters have been constructed [5] which require auxiliary storage. In one dimension, however, it is sufficient to use

$$\begin{aligned} \delta f_{j+1/2}^{n+1/2} \to S_{j+1/2} \cdot \max\{0, \min[& T_{j+1/2} \delta f_{j+1/2}^{n+1/2}, S_{j+1/2} \cdot (v_{j+2}^{n+1'} - v_{j+1}^{n+1'}), \\ & S_{j+1/2} \cdot (v_j^{n+1'} - v_{j-1}^{n+1'})]\}, \end{aligned} \tag{13}$$

where

$$\begin{aligned} S_{j+1/2} &= \operatorname{sign}(\delta f_{j+1/2}^{n+1/2}), \\ T_{j+1/2} &= \tfrac{1}{2}[S_{j+1/2} + \operatorname{sign}(v_{j+1}^{n+1'} - v_j^{n+1'})]. \end{aligned} \tag{14}$$

This is similar to the Boris-Book flux limiter, but with the following differences. The flux correction δf has been constructed as the difference between fluxes from two specified schemes, rather than the negative of a diffusive flux added to damp oscillations. The factor $T_{j+1/2}\delta f_{j+1/2}^{n+1/2}$ replaces $|\delta f_{j+1/2}^{n+1/2}|$ in the limiter of Ref. [1]. This replacement requires that the correction to high order not decrease gradients locally; i.e., the flux correction should be of an antidiffusive nature everywhere.

This form preserves monotonicity of v and results in total fluxes which are point-by-point *intermediate* between high and low order fluxes. The completed monotone pseudospectral update is then

$$v_j^{n+1} = v_j^{n+1'} - \delta f_{j+1/2}^{n+1/2} + \delta f_{j-1/2}^{n+1/2}. \tag{15}$$

This approach to flux limiting recovers the high order fluxes [5] $F_{j+1/2}$ at all locations $j+1/2$ except where the high order scheme could violate monotonicity at j or $j+1$. Thus spectral accuracy is retained in smooth regions.

Oscillations: Gibbs' Error and Phase Error

This section discusses properties of numerical schemes which have been recognized previously [15–17], but which have received little attention in the construction of flux limiters. Numerical oscillation is commonly attributed to Gibbs' error; i.e., the tendency of a series representation to oscillate near a jump in nodal values. A stronger contributor to numerical oscillation in advection scheme results is discretization error in phase and group speed. Numerical oscillations from difference schemes of various orders are illustrated in Fig. 1. (This figure is the first part of a before-and-after pair, with Fig. 4 containing results *after* flux correction. The pseudospectral results in Fig. 4 are flux-corrected in *exactly* the same way as the finite difference results.) Linear advection examples are given for two profiles which reveal numerical artifacts in finite difference schemes: a discontinuous square wave and a semicircle. The square wave tests monotonicity preservation and reveals residual numerical diffusion in the rounding of the discontinuity. The semicircle is sensitive to terracing or oscillation in slope.

A trademark of Gibbs' error is that the width, rather than the amplitude of the oscillation, tends to zero as the number of retained frequencies increases. The width of the region of spurious oscillations in Fig. 1, however, *increases* with the order of the scheme. This is characteristic of group velocity error. Figure 2 gives a result more typical of Gibbs' error. Here the linear advection example of Fig. 1e is carried much further in time with the pseudospectral method. A mild damping of the computational mode results from the leapfrog-trapezoidal time advancement scheme. As pointed out below, the pseudospectral method gives accurate phase speeds for all modes except the odd–even mode. Gradual removal of the small spectral interval where phase and group velocity errors are significant has exposed the underlying Gibbs' error.

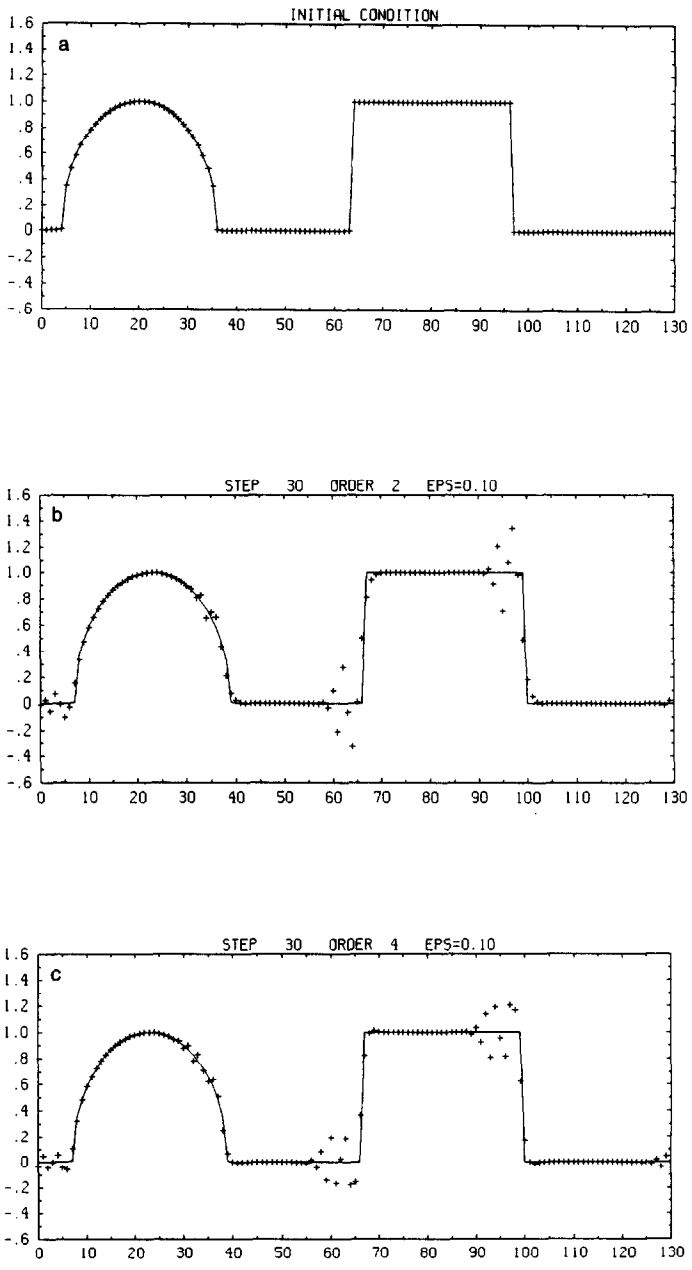

FIG. 1. Passive scalar advection test without flux limiter. (a) Initial condition; (b) Second order spatial differencing after 30 timesteps at a Courant number of 0.1; (c) Fourth order; (d) Eighth order; (e) Pseudospectral. Solid lines: analytic solution; points: numerical results.

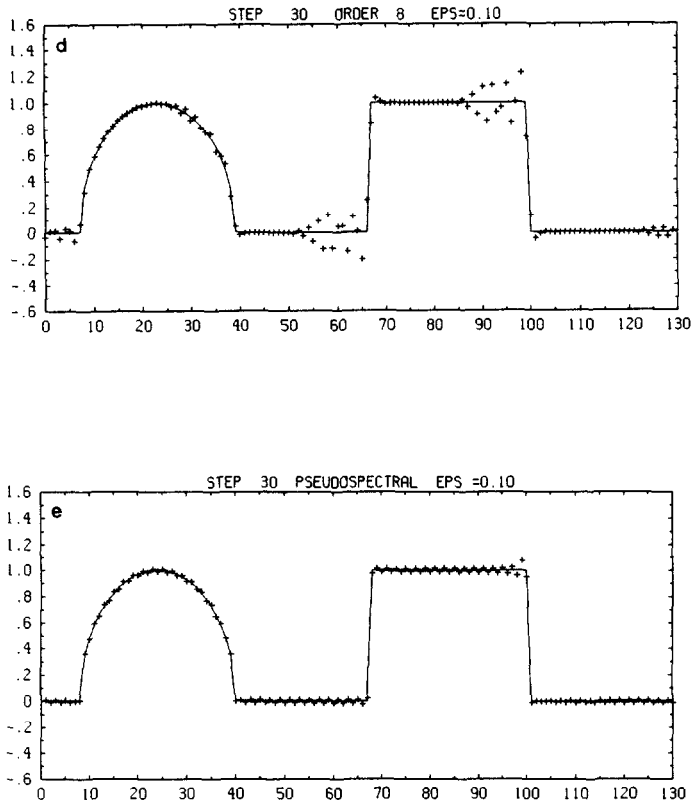

FIGURE 1—*Continued*

For the sake of illustration, Fig. 3 shows phase and group velocities for eight schemes of order 2 through 128 plus pseudospectral. Such high orders are included only to illustrate how much would be required of a finite difference scheme to challenge pseudospectral accuracy at high wavenumber. These curves are calculated to arbitrary order as follows. Consider the linear advection equation

$$\partial_t v = -c\partial_x v, \tag{16}$$

where c is constant. Assuming temporal and spatial variation $e^{i(kx-\omega t)}$ and replacing ∂_x in (16) with a finite diffeence operator of a given order accuracy then gives ω as a function of $k\,\delta x$. (Temporal truncation error is omitted from this analysis.) For a stable scheme of even order, ω is real. An expression for the numerical derivative of a function $f(x)$ accurate to order $2M$ at a point x_0 on an evenly spaced grid is [18]

$$\frac{\delta f(x_0)}{\delta x} = \sum_{i=-M\neq 0}^{M} \frac{f(x_i)-f(x_0)}{x_i-x_0} \prod_{j=-M\neq 0,\,i}^{M} \frac{j}{j-i}, \tag{17}$$

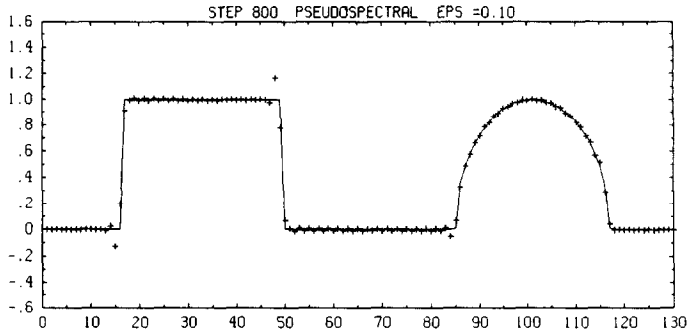

FIG. 2. Pseudospectral calculation of 1e continued to 800 steps.

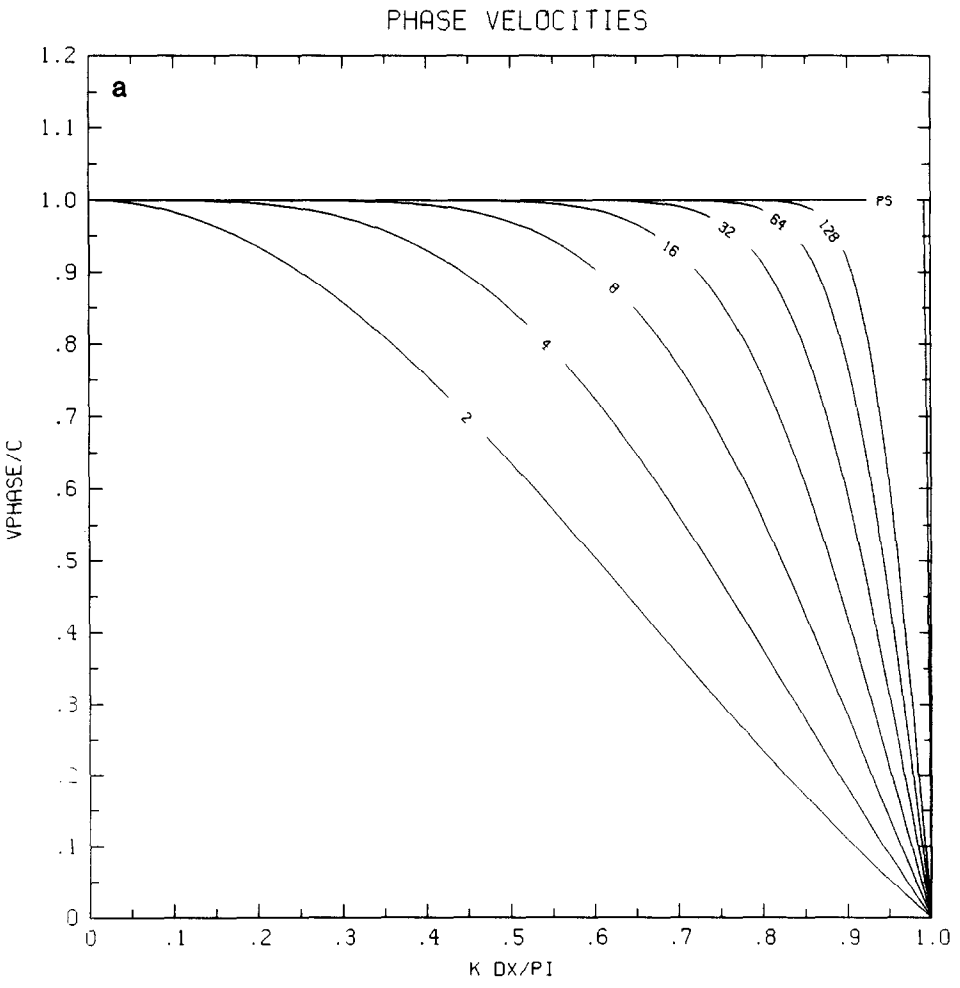

FIG. 3. (a) Phase and (b) group velocity normalized to true values as a function of the wavenumber for schemes of the indicated order.

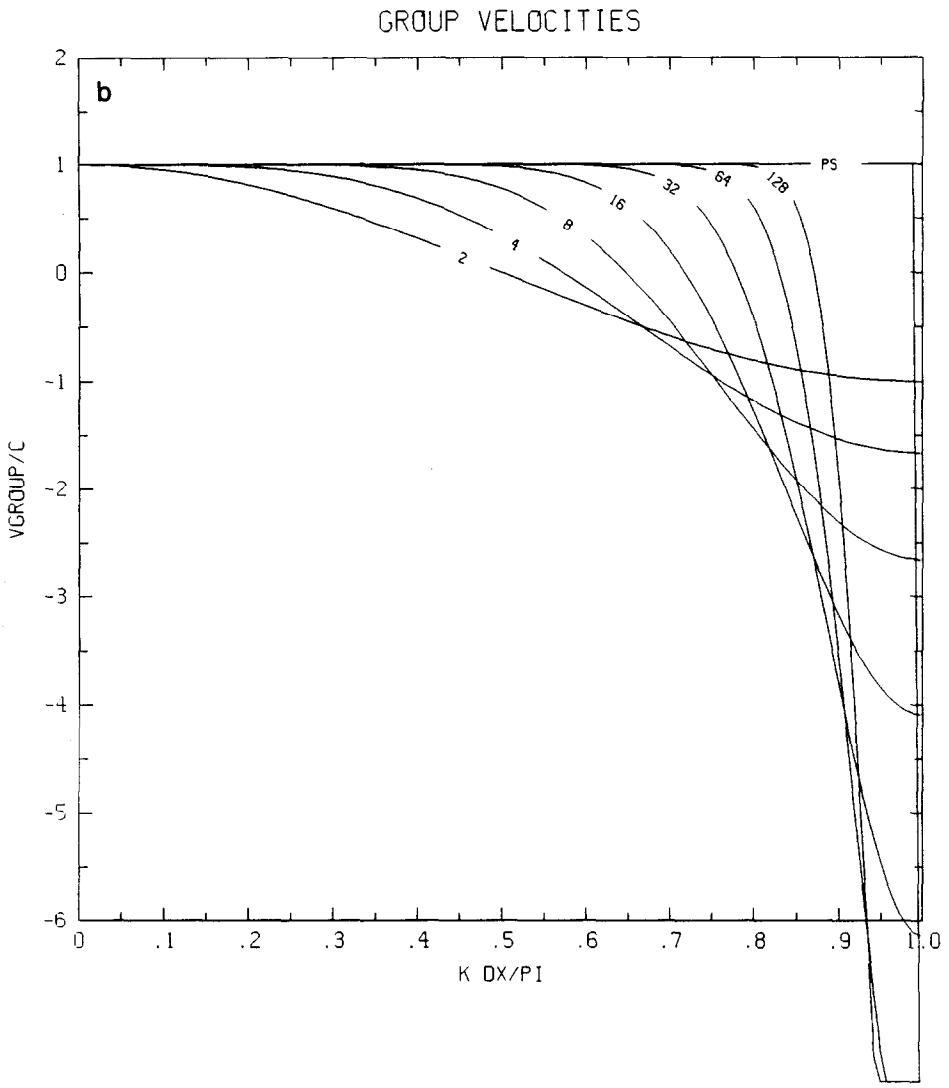

FIGURE 3—*Continued*

where x_0 resides at the center of the $2M+1$ point stencil $(x_{-M}, ..., x_M)$. Use of this result to calculate a dispersion curve from (16) leads to the following expressions for the phase velocities (18) and group velocities (19) for constant mesh spacing δx.

$$\frac{\omega}{ck} = \sum_{n=-M\neq 0}^{M} \frac{\sin nk\,\delta x}{nk\,\delta x} \prod_{j\neq 0,\,n} \frac{j}{j-n} \tag{18}$$

$$\frac{\partial_k \omega}{c} = \sum_{n=-M\neq 0}^{M} \cos nk\,\delta x \prod_{j\neq 0,\,n} \frac{j}{j-n}. \tag{19}$$

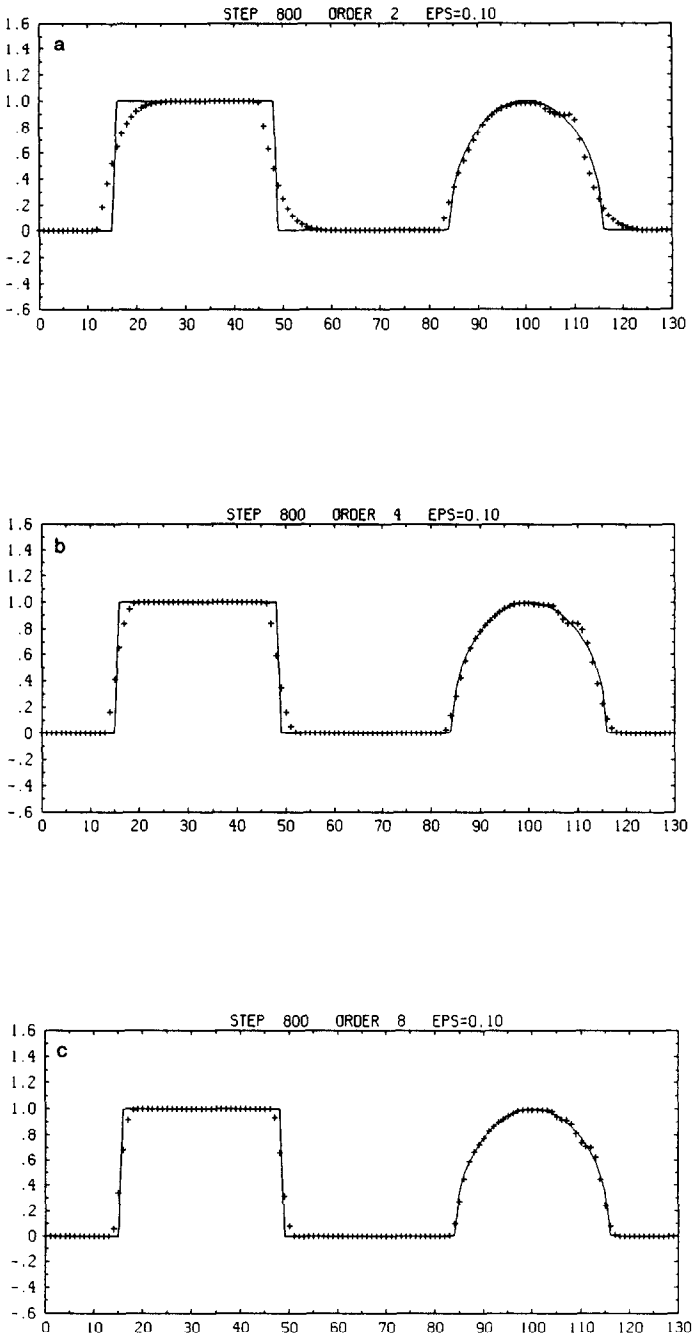

FIG. 4. Results analogous to Fig. 1 after 800 steps *including* the flux limiter of Eq. (13).

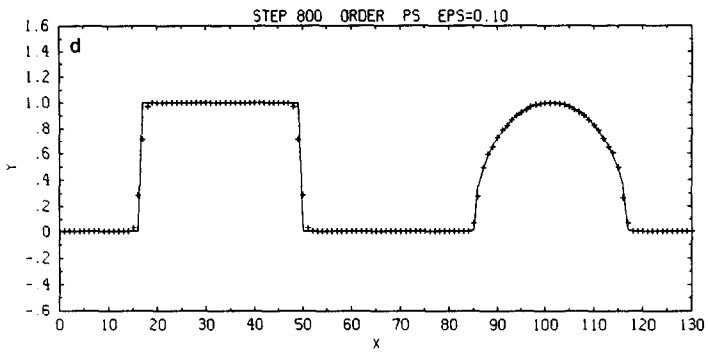

FIGURE 4—*Continued*

Figure 3 reflects that phase velocities from finite difference schemes are accurate for the well-resolved (low wavenumber) modes, but fall to zero at the odd–even mode. Then the best a *real* scheme can do is stay with the linear dispersion relation as long as possible before falling away. (In principle, a *complex* scheme could be constructed to retain phase information lost in time-advancing the odd–even mode.) Since the group velocity (i.e., the wave packet speed) is proportional to the slope of the dispersion curve $\omega(k)$, information in the high wavenumber modes propagates in the wrong direction at a speed which increases with increasing order. This behavior is evident in Fig. 1.

With the pseudospectral method, only the highest mode falls off the phase velocity curve, so that group velocities are accurate for all but the highest mode interval. The leapfrog-trapezoidal time advancement scheme used here contributes a mild damping to these modes, keeping results from being highly contaminated with the backward-running error seen in Fig. 1. Extension of the calculation of Fig. 1e from 30 to 800 timesteps with the pseudospectral method (Fig. 2) yields the low oscillation and high structure resolution levels one would hope for *before* applying a monotonicity filter.

An interesting and little-realized fact can be gleaned from Fig. 3. Even when the finite difference order is one less than the number of grid points, errors still occur in the high wavenumber phase and group velocities, and the pseudospectral method stands unsurpassed. In this case, the polynomial representing the finite difference scheme passes through *all* the nodal values, and one might be tempted to think that this situation could not be improved. The resolution of this apparent paradox is that finite differences do not give exact results for differentiation of the sinusoid used in *defining* phase velocity, while the pseudospectral method does.

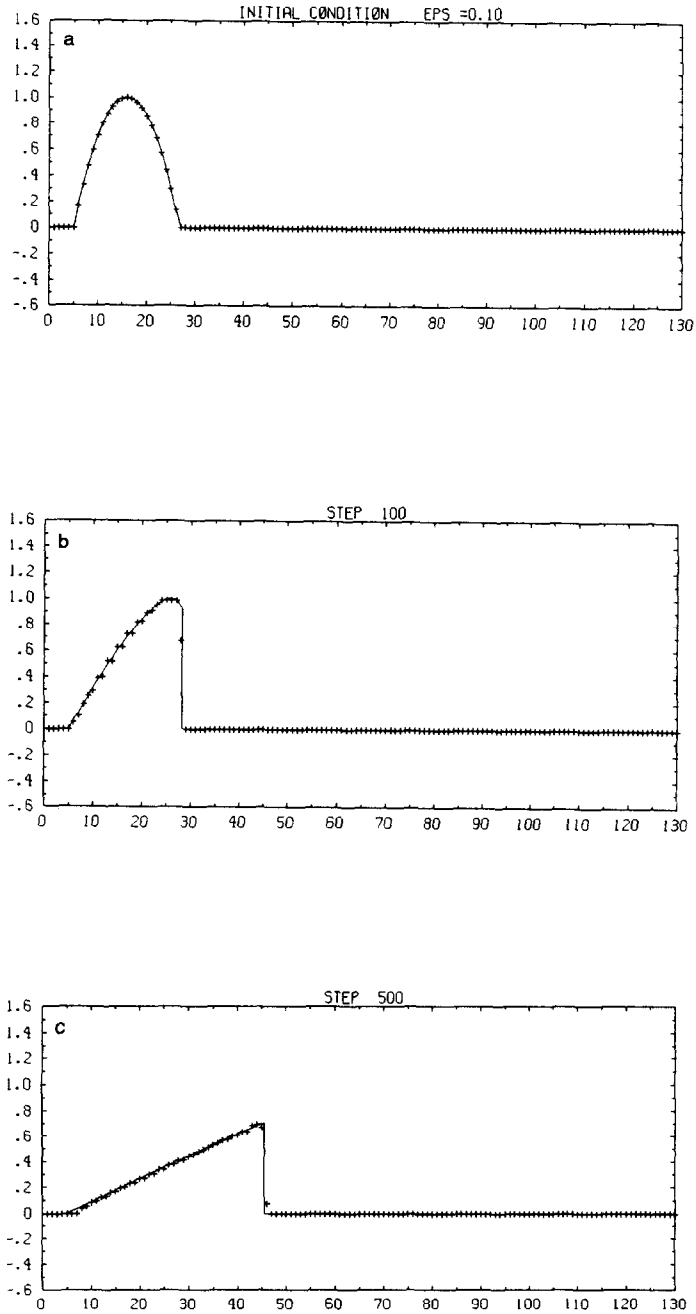

FIG. 5. Shock formation from Bergers' equation for an inverted parabolic profile initial condition. Solid line: analytic solution; crosses: PSF results.

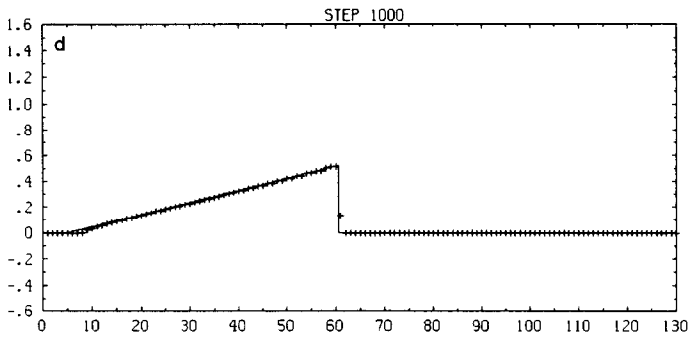

FIGURE 5—*Continued*

RESULTS WITH FLUX CORRECTION

Linear Advection

Figure 4 shows results analogous to those of Fig. 1 with a flux limiter of the form of (13) applied to finite difference methods of increasing order, including the scheme of (7)–(13). This latter combination will be designated PSF for pseudospectral flux correction. All tests use the leapfrog-trapezoidal time differencing scheme. Lacking the spurious oscillations of Fig. 2, Fig. 4 shows the kind of convergence with increasing order that one would hope to find in a well-behaved scheme. Numerical smoothing evident in the rounding and broadening of the step function profile decreases with order, even after the addition of the local diffusion implicit in the flux limiter.

A more demanding test of the schemes than monotonicity preservation is their accuracy against the formation of terraces. These result from the tendency to form oscillations in slope. These slope oscillations could occur at low amplitude without invoking any local smoothing from the flux limiter. Only when they reach an amplitude large enough to cause artificial extrema, the flux limiter enters and effectively converts an individual artificial extremum to a plateau. A distribution of these plateaus appears as a terrace. The semicircle profile of Fig. 4 shows a decreasing tendency to form terraces as the order of the scheme increases. Both the amplitude and width of the terraces decrease with order. This is consistent with the view that increasing the order of the scheme moves to a higher wavenumber and narrows the spectral interval over which phase and group velocities are in error.

Shock Formation

Another revealing test of a scheme for hyperbolic problems is to follow the evolution of a *continuous* profile subject to the inviscid Burgers' equation into steepening and shock propagation. Many tests of contemporary shock following methods have been published, in which shocks are present in *initial* conditions. These tests may

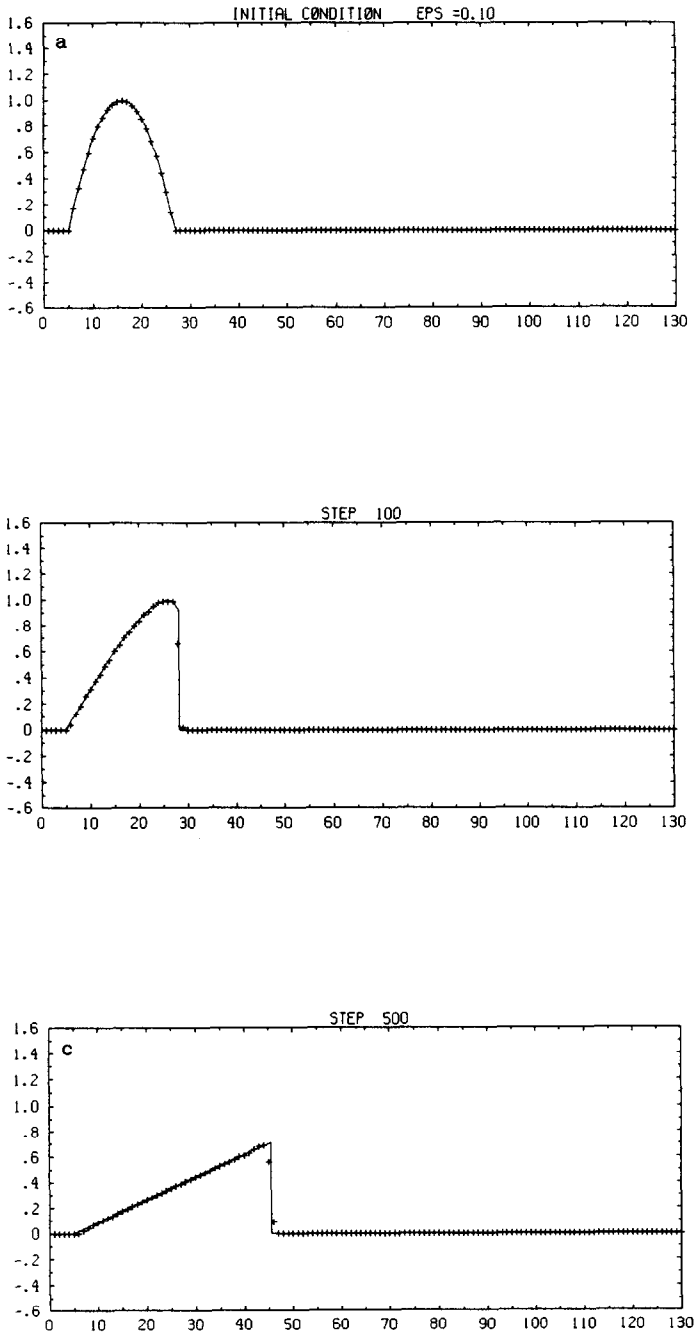

FIG. 6. The test problem of Fig. 5 with 16th order linear filter of (20).

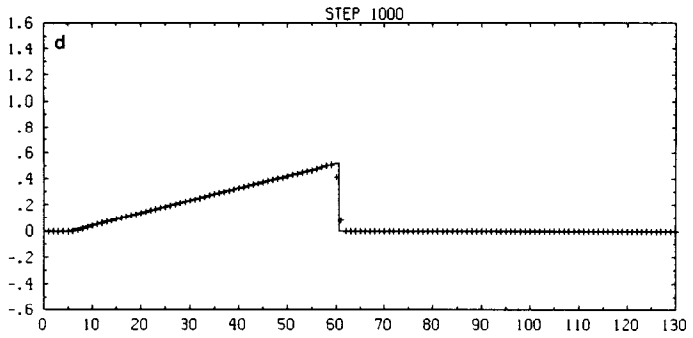

FIGURE 6—*Continued*

not reveal artifacts which can occur in the continuously steepening case. Pathologies that can occur in steepening have been demonstrated elsewhere [7].

Figure 5 shows PSF results for shock formation and propagation as described by the inviscid Burgers' equation, in comparison with the analytic solution. The shock front behavior is in excellent agreement with the analytic solution, while the back side of the shock is contaminated by an odd–even oscillation. This is substantially improved in Fig. 6 by the use of a high order (16th) linear filter. The filter consists of adding to (7) a flux

$$D_{j+1/2}^{n+1/2} = -\varepsilon \Delta^{m/2-1}(v_{j+1}^n - v_j^n), \tag{20}$$

where ε is the maximum Courant number in the calculation, $m = 16$, and Δ is the normalized second difference operator,

$$\Delta v_j \equiv -\tfrac{1}{4}v_{j+1} + \tfrac{1}{2}v_j - \tfrac{1}{4}v_{j-1}. \tag{21}$$

The filter (20) is added to the high order flux (7) *before* the flux limiter is evoked, so that monotonicity of the total scheme is preserved. This form for the filter was found most satisfactory after experimenting with several more complicated forms.

SUMMARY

Gibbs' error is often cited as the cause of numerical oscillation near discontinuities. It is likely, however, that finite difference phase error causes more artificial oscillation than Gibbs' error. The pseudospectral method is capable of higher quality resolution of discontinuities than finite difference schemes because of its accuracy in phase and group velocities for spatial modes below the Nyquist frequency. Numerical oscillations in both value and slope are smaller with the pseudospectral method than with finite difference schemes. The pseudospectral method when cast in flux difference form (7) is compatible with monotonicity-

enforcing flux limiters developed for finite difference schemes. The resulting pseudospectral flux correction (PSF) method appears very attractive for problems involving discontinuities and shock formation. For passive advection of a discontinuity at a uniform speed, PSF controls oscillations in value *and* slope while maintaining structure details. For shock propagation, however, a high-order linear filter is desirable for controlling oscillations in slope behind the shock. Further work is needed on this feature of the scheme.

ACKNOWLEDGMENTS

Work supported by the Office of Naval Research and Defense Nuclear Agency. Facilities of the Naval Research Laboratory/Laboratory for Computational Physics were of great value in completing this work. Discussions with J. Ambrosiano, J. P. Boris, D. L. Book, and S. T. Zalesak were helpful during the course of the work.

REFERENCES

1. D. GOTTLIEB, L. LUSTMAN, AND S. A. ORSZAG, *SIAM J. Sci. Stat. Comput.* **2**, 296 (1981).
2. M. Y. HUSSAINI AND T. A. ZANG, *Ann. Rev. Fluid. Mech.* **19**, 339 (1987).
3. S. A. ORSZAG, *Stud. Appl. Math.* **50**, 293 (1971).
4. J. P. BORIS AND D. L. BOOK, *J. Comput. Phys.* **11**, 18 (1971).
5. S. T. ZALESAK, *J. Comput. Phys.* **31**, 335 (1979).
6. S. T. ZALESAK, in *Proceedings, IMACS Symposium on Computer Methods for Partial Differential Equations-IV*, edited by R. Vichnevetsky and R. S. Stepleman (Rutgers Univ. Press New Brunswick, NJ, 1981), p. 126.
7. B. E. MCDONALD AND J. A. AMBROSIANO, *J. Comput. Phys.* **56**, 448 (1984).
8. T. D. TAYLOR, R. B. MYERS, AND J. H. ALBERT, *Comput. Fluids* **9**, 469 (1981).
9. B. ENGQUIST AND S. OSHER, *Math. Comput.* **14**, 45 (1980).
10. P. L. ROE, *J. Comput. Phys.* **73**, 357 (1983).
11. P. R. WOODWARD AND R. COLELLA, *J. Comput. Phys.* **54**, 174 (1984).
12. A. GRAMMELTVEDT, *Monthly Weather Rev.* **97**, 40 (1969).
13. B. E. MCDONALD, J. AMBROSIANO, AND S. ZALESAK, in *Proceedings, Eleventh IMACS World Congress, Oslo, Norway, 1985*, edited by R. Vichnevetsky (Rutgers Univ. Press, 1985), New Brunswick, NJ, p. 67.
14. E. TADMORE, ICASE Report 86-74, 1986 (unpublished).
15. R. C. Y. CHIN, G. W. HADSTROM, AND K. E. KARLSSON, *Math. Comput.* **33**, 647 (1979).
16. R. VICHNEVETSKY AND J. BOWLES, *Fourier Analysis of Numerical Approximations of Hyperbolic Equations* (SIAM, Philadelphia, 1982).
17. L. N. TREFETHEN, *SIAM Rev.* **24**, 113 (1982).
18. D. M. YOUNG AND R. T. GREGORY, *A Survey of Numerical Mathematics, Vol. 1* (Addison–Wesley, Reading, MA, 1972).